

# What Does the Gradient Tell When Attacking Graph Structure?

Zihan Liu<sup>1,2</sup>, Ge Wang<sup>2</sup>, Yun Luo<sup>2</sup>, Stan Z. Li<sup>2†</sup>

<sup>1</sup> Zhejiang University, Hangzhou, Zhejiang, China

<sup>2</sup> School of Engineering, Westlake University, Hangzhou, Zhejiang, China  
{liuzihan, stan.zq.li}@westlake.edu.cn

## ABSTRACT

Recent studies have proven that graph neural networks are vulnerable to adversarial attacks. Attackers can rely solely on the training labels to disrupt the performance of the agnostic victim model by edge perturbations. Researchers observe that the saliency-based attackers tend to add edges rather than delete them, which is previously explained by the fact that adding edges pollutes the nodes' features by aggregation while removing edges only leads to some loss of information. In this paper, we further prove that the attackers perturb graphs by adding inter-class edges, which also manifests as a reduction in the homophily of the perturbed graph. From this point of view, saliency-based attackers still have room for improvement in capability and imperceptibility. The message passing of the GNN-based surrogate model leads to the oversmoothing of nodes connected by inter-class edges, preventing attackers from obtaining the distinctiveness of node features. To solve this issue, we introduce a multi-hop aggregated message passing to preserve attribute differences between nodes. In addition, we propose a regularization term to restrict the homophily variance to enhance the attack imperceptibility. Experiments verify that our proposed surrogate model improves the attacker's versatility and the regularization term helps to limit the homophily of the perturbed graph.

## CCS CONCEPTS

• **Computing methodologies** → *Semi-supervised learning settings*.

## KEYWORDS

graph adversarial attack, gray-box poisoning attack, edge perturbation

## ACM Reference Format:

Zihan Liu<sup>1,2</sup>, Ge Wang<sup>2</sup>, Yun Luo<sup>2</sup>, Stan Z. Li<sup>2†</sup>. 2018. What Does the Gradient Tell When Attacking Graph Structure?. In *Proceedings of Make sure to enter the correct conference title from your rights confirmation email (Conference acronym 'XX)*. ACM, New York, NY, USA, 10 pages. <https://doi.org/xx.xx>

## 1 INTRODUCTION

Graph-structured data is widely used in real-world applications, such as social networks [8, 37], traffic networks [2, 30], and recommendation systems [33, 34]. Graph Neural Networks (GNNs)

[12, 15, 29], a family of deep learning frameworks, are broadly used due to their advantages in processing graph data [39]. In recent years, researchers have pointed out that inconspicuous perturbations on the graph structure can mislead the prediction of GNNs [6, 42]. As one of the mainstream approaches to test model robustness, the study of graph adversarial attacks has received more and more attention.

Graph Structure Attack (GSA) aims to misguide the model predictions by perturbing a limited number of edges. In the scenario of gray-box attack, the attacker generally constructs a surrogate model to carry out the attack and afterwards transfers the attack to unknown victim models [25]. One of the most popular attack methods on graph structure relies on gradient saliency from a constructed surrogate model [4, 16, 43]. Gradient saliency is proposed in the attribution domain, mining which input features are activated when the model is inferring [24, 27]. This approach is subsequently migrated to the field of adversarial attacks, demonstrating that the objective of adversarial attacks is likewise to disrupt these input features important for inference. There have been several attack models based on gradient saliency for the adversarial attack on the graph structure. Since the graph structure is discrete, edge perturbation attackers commonly refer to the gradient saliency on the graph structure and greedily modify the edges until the modification reaches the imperceptible limitation. Wu et al. [32] observe that saliency-based attackers following greedy algorithms constantly add edges instead of removing them. Subsequently, other researches have identified this phenomenon [11, 22, 28]. Wu et al. [32] explains that the attacker tends to connect nodes with high feature dissimilarity and uses this as a basis to propose the removal of edges between low similarities as a defensive measure. Tang et al. [28] extend the interpretation of [32]. They argue that adding edges tends to pollute the sharply transmitted information, yet deleting edges only leads to the loss of some information.

We are aware of the contact between GSA and the graph homophily inspired by the recent research in heterophily graphs [1, 21, 41]. Graph homophily captures the proportion of intra-class and inter-class edges. The information aggregation mechanism of GNNs leads to oversmoothing between two nodes connected by an edge [3, 13, 38]. It has the advantage of extracting low-frequency information of connected similar nodes through intra-class edges [1]. However, inter-class edges render the aggregation mechanism a burden. The information fusion between nodes from different classes causes the local subgraph to deviate from the distribution manifold, thus causing instability in the training process. We analyze and empirically validate that saliency-based poisoning attacks, such as Metattack [43], and exploit this property to express the effectiveness of the attack. Under the greedy algorithm, saliency-based attackers always choose to reduce the homophily of the perturbed graph by adding inter-class edges. Moreover, as mentioned

Permission to make digital or hard copies of all or part of this work for personal or classroom use is granted without fee provided that copies are not made or distributed for profit or commercial advantage and that copies bear this notice and the full citation on the first page. Copyrights for components of this work owned by others than ACM must be honored. Abstracting with credit is permitted. To copy otherwise, or republish, to post on servers or to redistribute to lists, requires prior specific permission and/or a fee. Request permissions from [permissions@acm.org](mailto:permissions@acm.org).  
Conference acronym 'XX, June 03–05, 2018, Woodstock, NY

© 2018 Association for Computing Machinery.  
ACM ISBN 978-1-4503-XXXX-X/18/06...\$15.00  
<https://doi.org/xx.xx>

in [32], the nodes connected by the attacker tend to differ significantly in their features. It is these added inter-class edges that explain the effectiveness that the attack exhibits after the model is retrained. The phenomenon that nodes with a high degree are less vulnerable to attacks [42] can also be explained by the local homophily of these nodes being more difficult to reduce.

For GNNs based on information aggregation, inter-class edges fuse the hidden features of nodes from different classes. It is this property that attackers exploit to carry out their attacks. However, the aggregation of nodes' features leads to oversmoothing between neighboring nodes, which means that the differential information of nodes is attenuated in the forward aggregation process. Since saliency-based attackers rely on backpropagation, the diversity of node attributes lost in the forward process is not reflected at the backpropagated gradient saliency. We argue that the surrogate model, which is used to provide gradient saliency, should have the performance of the downstream task and the nodes' original high-frequency information in the forward process. To demonstrate this proposition, we propose multi-hop aggregation to enhance the forward mapping of the surrogate model. We isolate the low- and high-frequency information at different aggregation levels and retain them separately in the forward process. This improvement enriches the information on the saliency map, thus helping attackers to find more effective attack strategies.

On the other hand, the saliency-based attacker's propensity to add inter-class edges produces a decreasing trend for the homophily of the perturbed graph. Inspired by this, we ponder whether we could suppress this trend to improve the attack imperceptibility, while we are curious about how much attack performance the model could exhibit while limiting the decrease in homophily. To this end, we propose a regularization term that can implicitly guide the attacker to balance the graph homophily by affecting the gradient saliency on the graph structure. Since the labels of the test nodes are invisible, we employ pseudo-labels to strictly limit the homophily of the attacker on the surrogate model. When the attack is transferred to the victim model, the regularization term performs to decelerate the homophily decrease. We design rich experiments to verify the improvement of the optimization of our proposed surrogate model and the attacker's performance when the decrease of graph homophily is restricted.

The main contribution of this paper is summarized as follows.

- We analyze that saliency-based attackers tend to add inter-class edges, leading to a decrease in homophily, which provides a reasoning for the attack performance of such attackers.
- We point out that the aggregation of GNNs causes difficulties for saliency-based attackers to exploit nodes' high-frequency information. We propose the multi-hop aggregation for the surrogate model to preserve this information in gradient saliency.
- We propose a regularization term that decelerates the decline in homophily, in order to improve imperceptibility as well as to probe the attacker's attack performance under the homophily constraint.

## 2 RELATED WORK

There are various settings of graph adversarial attack depending on the attacker's knowledge, target, and attack scenario [35]. The

attacker's knowledge classifies the researches into white-box attack [32, 36], gray-box attack [32, 43] and black-box attacks [6, 18]. In the gray-box attack, which is the setting in this paper, the training set labels are visible to the attacker. The attacker's target include targeted attack [6, 42] and untargeted attack [14, 43]. Attack models can be further classified into the evasion attack and poisoning attack according to the attack scenario. The evasion attacks do not retrain the victim model after the perturbation, which is generally studied in white-box attacks [32, 36]. In contrast, poisoning attacks retrain the victim model, so the attacker focuses on the attack's transferability with respect to vulnerable nodes and graph structures [26, 43]. The existing attack methods are divided into two main categories: graph modification attack (GMA) and graph node injection (GNI) [10]. GMA only allows an attacker to change the properties of existing nodes and the connections between them [14, 17]. Most studies are devoted to attacking GNNs by modifying the graph structure only, which is denoted by graph structure attack (GSA).

Several GSA researchers have analyzed and interpreted the attack performance and the propensity of the attack model. Zugner et al. mention in [42] that high-degree nodes have better accuracy in both the clean and perturbed graphs. Wu et al. [32] observe that the saliency-based attackers tend to add edges rather than delete edges. Xu et al. [36] point out that part of the attacker's budget is allocated to nodes that have been misled and propose a Carlisle-Wagner-type loss. Geisler et al. [7] collate the attack loss and suggest that the attack loss based on cross-entropy is unreasonable. As the propensity for attacks continues to be discovered, many efforts have expressed concern about the imperceptibility of the attacks [4, 25]. GSA is generally restricted by the  $\ell_0$  norm of the change in the adjacent matrix. Dai et al. [6] propose to utilize a benchmark GNN as an evaluation criterion for imperceptibility in white-box attacks. Ma et al. [18] propose a rewiring approach to attack graph structure in graph classification problems and discusses its ability to improve the imperceptibility of the attack by reducing the impact of perturbations on the eigenvalue of the graph Laplacian matrix. Chen et al. [5] notice the importance of homophily in GNI and restrict the homophily calculated by the inner product of node features. Similar to [5], this paper demonstrates the tendency of homophily decline in GSA and proposes a plug-and-play homophily regularization term applied to saliency-based attackers.

## 3 PRELIMINARIES

### 3.1 Notations

For a attribute graph  $\mathcal{G}$ , it can be represented as  $\mathcal{G} = (\mathcal{V}, \mathcal{E}, X)$ , where  $\mathcal{V} = \{v_1, v_2, \dots, v_n\}$  is the set of  $N$  nodes,  $\mathcal{E} \subseteq \mathcal{V} \times \mathcal{V}$  is the edge set. GNNs are expected to predict the class of unlabeled nodes using the known labels in node-level classification tasks under semi-supervision. The attribute graph has a node feature matrix  $X$  and a subset of the labeled nodes with the label set of  $Y$ . Each sample is mapped as a node  $v_i$  on the graph with its feature  $x_i \in \mathbb{R}^d$  and label  $y_i \in \mathbb{R}^k$ , where  $k$  is the number of classes. A binary adjacent matrix  $A \in \{0, 1\}^{N \times N}$  is denoted to describe the edges between nodes, where  $A_{i,j} = 1$  if  $(i, j) \in \mathcal{E}$ . The mapping function of a GNN model is noted as  $f_\theta$ , while the prediction of  $f_\theta$

on each node  $v_i$  is represented by a distribution  $z_i$ . All the notations with  $\mathcal{L}$  denote the loss functions. Specific to attacks via edge perturbation, the perturbed graph is indicated as  $\mathcal{G}^{(t)} = (A^{(t)}, X)$ , where  $t$  represents the  $t$ -th time the attacker greedily modifies an edge in the graph.

### 3.2 Limitation of Attack

This paper focuses on the graph adversarial attack by edge perturbation. For the edge perturbation on an undirected graph, its perturbation is limited by the attack budget  $\Delta$ , whose mathematical expression is:

$$\|A^{(t)} - A^{(0)}\|_0 \leq 2\Delta, \quad (1)$$

where  $\|\cdot\|_0$  denotes the  $\ell_0$  norm function. Attacks on the graph structure only change a small number of edges and are therefore relatively invisible.

## 4 METHODOLOGY

In Section 4.1, we introduce the attack pipeline of the saliency-based edge perturbation attacker. In Section 4.2, we theoretically analyze the phenomenon that saliency-based attackers tend to add inter-class edges. In Section 4.3, we propose that the discrepancy information of nodes' attributes is lost in the forward process due to the message passing mechanism of GNNs. We propose a novel surrogate model to solve this problem. In Section 4.4, we highlight the effect of adding inter-class edges on the graph homophily. We propose a novel attack loss that can constrain the homophily of perturbed graphs, aiming to explore the relationship between attack performance and homophily and ways to enhance attacks' imperceptibility.

### 4.1 Saliency-based Attack Model

Due to the sparsity and discreteness of the graph structure, attackers cannot follow the example of Projected Gradient Descent (PGD) [19] with superimposed saliency. Under the constraint elaborated by Equation (1), Zugner et al. first propose a greedy algorithm for the attack model [43]. The greedy algorithm makes the attacker adopt only the edge with the most significant gradient values as the perturbation in each call to the saliency map. Each perturbation is considered a bi-level optimization problem in which the model is retrained on the perturbed graph and generates perturbations for the next stage. Greedy edge perturbation at each stage is formulated as:

$$\begin{aligned} A^{(t)} &= \min_{\|A^{(t)} - A^{(t-1)}\|_0 = 2} \mathcal{L}_{atk}(f_{\theta^{(t)}}(A^{(t)}, X)) \\ \text{s.t. } \theta^{(t)} &= \underset{\theta}{\operatorname{argmin}} \mathcal{L}_{train}(f_{\theta}(A^{(t-1)}, X), Y), \end{aligned} \quad (2)$$

where  $\theta^{(t)}$  denotes the parameter matrices of the surrogate model by minimizing a cross-entropy training loss  $\mathcal{L}_{train}$ . The general form of  $f_{\theta}$  is a standard Graph Convolutional Network (GCN):

$$f_{\theta}(A, X) = \operatorname{softmax}(\hat{A}\sigma(\hat{A}XW^{(0)})W^{(1)}), \quad (3)$$

where  $\hat{A} = \tilde{D}^{-\frac{1}{2}}(A + I)\tilde{D}^{-\frac{1}{2}}$  is the normalized adjacent matrix. At stage  $(t)$ , the attacker selects one edge to modify (two for adjacency matrix due to symmetry), targeting to minimize the attack loss  $\mathcal{L}_{atk}$ . There are formats of  $\mathcal{L}_{atk}$ , such as cross-entropy [43],

minmax [36]. In this paper,  $\mathcal{L}_{atk}$  is set as a cross-entropy loss, which is formulated as:

$$\mathcal{L}_{atk} = -\mathcal{L}_{ce}(f_{\theta^{(t)}}(A^{(t)}, X), Y'_{test}), \quad (4)$$

where  $Y'_{test}$  is the pseudo-label of  $f_{\theta^0}(A^{(0)}, X)$  (i.e., the model trained from the clean graph). The iterations continue until the perturbed graph satisfies  $\|A^{(t)} - A\|_0 = 2\Delta$ . Minimizing  $\mathcal{L}_{atk}$  is not a problem that can be solved by a forward process. As an approximation, the gradient saliency, which is back-propagated through the attack loss, reflects the expectation of modification to the variation in  $\mathcal{L}_{atk}$ . The calculation of gradient saliency on the adjacent matrix  $A^{(t)}$  is following:

$$\mathcal{A}^{(t)} = \nabla_{A^{(t)}} \mathcal{L}_{atk}(f_{\theta^{(t)}}(\mathcal{G}^{(t)})), \quad (5)$$

where  $\mathcal{A}^{(t)}$  denotes the gradient saliency at stage  $(t)$ , and  $\nabla$  denotes the gradient operator.

On the graph structure, the edges take the value 0 or 1, which means that the perturbation can only cause the edge to change to a determined state. When the value of an edge is 0, a positive gradient value means that adding this edge is a sound attack strategy; conversely, a negative gradient value means that removing this edge is a sound attack strategy. The attacker greedily selects the edge with the most significant absolute gradient value from the sound attack strategy as the perturbation. The expression for the perturbation at the moment  $(t+1)$  based on the gradient saliency at the moment  $(t)$  is:

$$A^{(t+1)} - A^{(t)} = \underset{(i,j)}{\operatorname{argmax}} \mathcal{A}_{i,j}^{(t)} (1 - 2A_{i,j}^{(t)}), \quad (6)$$

where  $(1 - 2A^{(t)})$  converts the edge state from (0,1) to (1,-1) aims to weight the gradient saliency. Note that at every iteration the adjacent matrix is modified simultaneously at symmetrical position, i.e.,  $\|A^{(t+1)} - A^{(t)}\|_0 = 2$ . The attack process ends at the  $\Delta^{th}$  iteration when  $A^{(t)}$  satisfies  $\|A^{(t)} - A^{(0)}\|_0 = 2\Delta$ .

### 4.2 What are Saliency-based Attackers Looking for?

We have interpreted how saliency-based attackers utilize gradient saliency on the graph structure by Equation (2)-(6). This section discusses the gradient saliency to dig deeper into the tendencies of attacks.

We first construct a sub-graph scenario, as shown in Figure 1. We assume that the label propagation algorithm (LPA) is used to infer the label of the intermediate target node (in green). The target node is connected to  $n_1$  nodes of class 1 and to  $n_2$  nodes of class 2. Suppose  $n_1 > n_2$ , according to LPA, the target node has the same label as the dominant category of its neighbors, i.e., class 1, and its prediction confidence is  $\frac{n_1}{n_1+n_2}$ . Subsequently, we assume that the edges are non-discrete and try to maximize the probability of the target node being classified as class 1 with a perturbation of size  $\delta$ . This small perturbation can be applied to the graph in four approaches: to reduce the weight of an edge connected to a node of class 1 or 2; to connect to a node of class 1 or 2 that is not connected. Among these, we can easily distinguish that  $\delta_{(1)}$ : adding an edge connected to a class 2 node with weight  $\delta$ , and  $\delta_{(2)}$ : reducing the weight of an edge connected to class 1 to  $1 - \delta$  are the

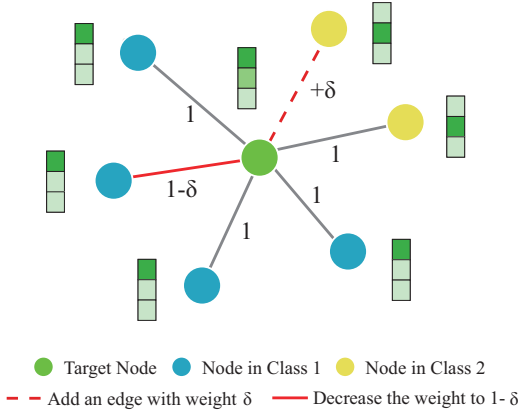


**Figure 1: Illustration of the gradient-based attack method.**  $\delta$  is a minimal amount of perturbation that aims to minimize the prediction confidence on the target node. It can create an edge with weight  $\delta$ , or it can decrease the weight of an existing edge to  $1 - \delta$ .

only two perturbations that can reduce the prediction confidence of the target node. The influence of the two perturbations on the target node's prediction confidence is:

$$p(\delta_{(1)}) = \frac{n_1}{n_1 + n_2 + \delta}, \quad p(\delta_{(2)}) = \frac{n_1 - \delta}{n_1 - \delta + n_2}, \quad (7)$$

where  $p(\cdot)$  denotes the prediction confidence at class 1. To compare the attack performance of  $\delta_{(1)}$  and  $\delta_{(2)}$ , we calculate the difference in prediction confidence due to the two perturbations in Equation (7). The result of the mathematical expression for  $p(\delta_{(1)}) - p(\delta_{(2)})$  is simplified as:

$$p(\delta_{(1)}) - p(\delta_{(2)}) = \frac{\delta n_2 - \delta n_1 + \delta^2}{(n_1 + n_2)^2 - \delta^2}. \quad (8)$$

If  $\delta \rightarrow 0$ , then we have  $p(\delta_{(1)}) < p(\delta_{(2)})$ . Notice that gradient saliency can be interpreted as the effect of the individual parameters on the objective, reducing prediction confidence in Figure 1.

**LEMMA 1.** Let  $P_{\mathcal{L}, \delta a}(k)$  be a perturbation function which is defined as  $P_{\mathcal{L}, \delta a}(k) \equiv \mathcal{L}(a_0, \dots, a_k + \delta a, \dots, a_D) - \mathcal{L}(a_0, \dots, a_k, \dots, a_D)$ , where  $a_k$  denotes the  $k^{\text{th}}$  dimension and  $\mathcal{L}$  denotes the attack target function. Then, if  $\argmin_k (P_{\mathcal{L}, \delta a}(k)) = d$ , the gradient of  $\mathcal{L}(a_0, \dots, a_k, \dots, a_D)$  w.r.t  $a$  has the minimum at  $d^{\text{th}}$  dimension of  $a$ .

**PROOF.** According to the property of  $\argmin$ , for a positive scalar  $\delta a$ , we have

$$\argmin_k \left( \frac{P_{\mathcal{L}, \delta a}(k)}{\delta a} \right) = d$$

The inner part of  $\argmin$  can be viewed as the partial derivative, i.e.,

$$\begin{aligned} \frac{P_{\mathcal{L}, \delta a}(k)}{\delta a} &= \frac{\mathcal{L}(a_1, \dots, a_k + \delta a, \dots, a_D) - \mathcal{L}(a_1, \dots, a_k, \dots, a_D)}{(a_k + \delta a) - (a_k)} \\ &\equiv \frac{\partial \mathcal{L}(a_1, \dots, a_k, \dots, a_D)}{\partial a_k} \equiv (\nabla_a \mathcal{L})_k \end{aligned}$$

Thus, the gradient of  $\mathcal{L}(a_1, \dots, a_k, \dots, a_D)$  w.r.t  $a$  has the minimum at  $d^{\text{th}}$  dimension of  $a$ .

According to Lemma 1, the sub-graph in Figure 1 results in a larger gradient saliency on the unconnected edge to nodes from class 2 (shown by the red dashed line) than a well-connected edge to a node from class 1 (shown by the solid red line). Thus, as stated in proposition 1, for an idealized graph, the optimal attack strategy generated by an attacker based on gradient saliency tends to add edges that connect nodes with different labels.

**PROPOSITION 1.** For a class of edge perturbation function  $P = \{p | p : A \rightarrow A\}$ ,  $A = \{A_{n \times n} | A_{i,j} \in \{0, 1\}\}$ , the optimal perturbation function follows  $p^* = \argmax_{p \in P} \mathcal{L}(p(A))$ . The optimal policy found by the saliency-based attacker obeys:

$$p^* = \begin{cases} A_{i,j} + 1 & , \text{ if } (i, j) \notin \mathcal{E} \text{ \& } y_i \neq y_j \\ A_{i,j} & , \text{ o.w.} \end{cases}$$

We abstractly represent the disruption of model performance in terms of  $\argmax \mathcal{L}$ . This expression can also be replaced by  $\argmin \mathcal{L}_{atk}$  that the perturbations promote the fitting of the attack loss. Attacking a real-world graph dataset is a non-idealized scenario. First, real-world graph datasets suffer from label noise. Mislabeling leads to significant feature differences between intra-class nodes, which exhibit contamination of neighboring nodes after information aggregation. Second, the attack on the real-world dataset is restricted to  $p : A \rightarrow A^{(2\Delta)}$ , which allows only a few highly significant edges to be perturbed. As a result, saliency-based edge perturbation manifests itself in real graph attack scenarios as a high probability of adding the inter-class edges.

### 4.3 Enhancing the Attacker's Sensitivity to Node Attributes

The tendency of saliency-based attackers to add inter-class edges has been illustrated in Section 4.2. This has a visible effect on the model's gradient saliency of the nodes' probability distribution output. In addition, we consider that the difference in attributes between nodes is an essential reference for the attacker. Edges connecting nodes with significant differences in attributes are more likely to pass contaminative neighbor features to both sides of the edge. However, the message passing mechanism of graph neural networks destroys the original attribute differences between nodes. Message passing of Graph Convolutional Network (GCN):

$$X^{(t+1)} = \tilde{D}^{-\frac{1}{2}} \tilde{A} \tilde{D}^{-\frac{1}{2}} X^{(t)}, \quad (9)$$

where  $\tilde{A} = A + I$  and  $\tilde{D}_i = \sum_j A_{ij}$ . We can rewrite GCN as:

$$X^{(t+1)} = (I - L_{sym}) X^{(t)}, \quad (10)$$

where  $L_{sym} = \tilde{D}^{-\frac{1}{2}} \tilde{L} \tilde{D}^{-\frac{1}{2}}$ , where  $L_{sym} = \tilde{D}^{-\frac{1}{2}} \tilde{L} \tilde{D}^{-\frac{1}{2}}$ ,  $\tilde{L} = \tilde{D} - \tilde{A}$ .

**THEOREM 2.**  $\mathcal{G}$  is a non-bipartite and connected graph with  $n$  nodes  $\mathcal{V} = \{v_1, \dots, v_n\}$ , and  $X_i^{(0)}$  is the attribute of node  $v_i$ . Then for  $\tau$  large enough, after  $\tau$  times message passing,  $\|X_i^{(\tau)} - X_j^{(\tau)}\|_2 \leq \|X_i^{(0)} - X_j^{(0)}\|_2$ .

PROOF. Let  $(\lambda_1, \dots, \lambda_n)$  and  $(e_1, \dots, e_n)$  denote the eigenvalue and eigenvector of matrix  $I - L_{sym}$ , respectively. According to the property of symmetric Laplacian matrix for connected graph.

$$-1 < \lambda_1 < \lambda_2 < \dots < \lambda_n = 1$$

$$e_n = \tilde{D}^{-\frac{1}{2}} [1, 1, \dots, 1]^T$$

We can rewrite  $X_i^\tau - X_j^\tau$  as:

$$X_i^{(\tau)} - X_j^{(\tau)} = [(I - L_{sym})^\tau X]_i - [(I - L_{sym})^\tau X]_j$$

$$= [\lambda_1^\tau (e_1^{(i)} - e_1^{(j)}), \dots, \lambda_{n-1}^\tau (e_{n-1}^{(i)} - e_{n-1}^{(j)}), \lambda_n^\tau (e_n^{(i)} - e_n^{(j)})] \tilde{X}$$

$e_k^{(i)}$  is the  $i^{th}$  element of eigenvector  $e_k$ ,  $\tilde{X}$  is the coordinate matrix of  $X$  in the space spanned by eigenvectors  $(e_1, \dots, e_n)$ . Thus,

$$X_{||i-j||}^{(\tau)} := \|X_i^{(\tau)} - X_j^{(\tau)}\|_2 = \sqrt{\sum_{m=1}^p \left[ \sum_{k=1}^n \lambda_k^\tau (e_k^{(i)} - e_k^{(j)}) \tilde{X}_{km} \right]^2}$$

Because  $-1 < \lambda_1 < \lambda_2 < \dots < \lambda_{n-1} < 1$ , thus for a large  $\tau$ ,  $X_{||i-j||}^{(\tau)} < X_{||i-j||}^{(0)}$ .

Further analysis of the variation of the difference between the two nodes is presented in Appendix A.

Theorem 2 demonstrates that the attribute differences between nodes tend to shrink during information aggregation. This narrowing is not of equal magnitude for all node pairs but is specific to the eigenvector. As the information is forwarded through GCNs, the differences in attributes between nodes are gradually reduced and distorted. The loss of information in the forward process causes the back-propagated gradients not to contain the lost information. This prevents salience-based attackers from exploiting their strengths properly.

We propose a multi-hop aggregation-based surrogate model to address the problem of losing attribute difference information due to message passing. The  $l$ -th layer of a multi-hop aggregation model consists of  $L$  layers following the form:

$$H_l^{(i)} = \text{CONCAT}[H_{l-1}^{(i)}, (\hat{A}H_{l-1})^{(i)}, (\hat{A}^2H_{l-1})^{(i)}]W^{(l-1)}, \quad (11)$$

where  $H_l^{(i)}$  represents the representation of node  $v_i$  at layer  $l$ ,  $\text{CONCAT}$  represents the concatenate operation, and  $W$  denotes learnable matrices. During the mapping process at the  $l-1^{th}$  layer,  $H_{l-1}^{(i)}$  is responsible for propagating the differentiation (high frequency) information of the nodes to the  $l^{th}$  layer.  $(\hat{A}H_{l-1})^{(i)}$  and  $(\hat{A}^2H_{l-1})^{(i)}$  extract various levels of low-frequency information, i.e., hidden representation after first-order and second-order aggregation. Equation 11 allows information from high to low frequencies to be preserved during the forward process. Thus, the surrogate model has both discriminative performances and preserves the differentiation of nodes from the input space.

#### 4.4 Enhancing the Attacker's Imperceptibility in Homophily

Section 4.2 has shown that saliency-based attackers tend to add inter-class edges. A corollary of this phenomenon is an observable decrease in the homophily of the graph structure. Graph homophily is a property of the node-level classification task, which reflects the degree of reliability of the graph structure.

The graph homophily  $h$  of a given graph  $G$  is defined as the proportion of edges in the graph that connects nodes with the same class label (i.e., intra-class edges), which is defined as:

$$h = \frac{|\{(i, j) : (i, j) \in \mathcal{E} \wedge y_i = y_j\}|}{|\mathcal{E}|}, \quad (12)$$

where  $y_i$  is the ground-truth or pseudo labels of node  $v_i$ . Graphs with strong homophily have a high homophily ratio  $h \rightarrow 1$ , while graphs with strong heterophily (i.e., weak homophily) have a small homophily ratio  $h \rightarrow 0$ . Additionally, graphs with a high homophily ratio are termed homophily/assortative graphs, and on the contrary, graphs with a low homophily ratio are termed heterophily/disassortative graphs.

Note that the homophily  $h$  is related to the label set  $Y$  and the edge set  $\mathcal{E}$  (i.e., the adjacent matrix  $A$ ). We define the homophily ratio of the original graph as  $h_Y(A)$  and the homophily ratio of the perturbed graph as  $h_Y(A^\Delta)$ . When the vast majority of perturbations are adding interclass edges, the expression for the homophily ratio of the perturbation graph is:

$$h_Y(A^\Delta) = h_Y(A) \frac{|\mathcal{E}|}{|\mathcal{E}| + \Delta} \quad (13)$$

The decrease in the homophily ratio of the perturbed graph relative to that of the original graph is:

$$h_Y(A) - h_Y(A^\Delta) = h_Y(A) \frac{\Delta}{|\mathcal{E}| + \Delta} \quad (14)$$

Researches on graph homophily have found that lower homophily tends to imply poorer classification performance because information aggregation introduces significant noise from neighboring nodes [41]. In terms of the saliency-based edge perturbation, we ask two questions:

- Is there a necessary connection between attack performance and the decline in graph homophily?
- If the decline in homophily is restricted, can the attacker still exhibit attack performance?

To answer the above questions and to uncover whether saliency-based attackers can exhibit the ability to attack with smaller variations of homophily, we propose a novel attack loss.

The gray-box attack setting limits the agnostic nature of the victim model. Besides, the ground-truth labels of the test nodes are unknown for both the attacker and the victim model. Thus, the graph homophily should be calculated from the ground-truth labels of the training nodes and the model-specific pseudo-labels of the test nodes. The homophily of the original graph is denoted as  $h_{\hat{Y}}(A)$  and the homophily of the perturbed graph is denoted as  $h_{\hat{Y}}(A^\Delta)$ , where  $\hat{Y} = Y_{train} \cup Y'_{test}$ , and  $Y'_{test}$  denotes the pseudo-labels of test nodes. The attacker simulates the case on the victim model with the surrogate model. We expect the decrease in graph

homophily of the surrogate model to be restricted by a proportionality parameter  $\varepsilon$ , denoted as

$$h_{\hat{Y}}(A) - h_{\hat{Y}}(A^\Delta) \leq \varepsilon h_{\hat{Y}}(A), \quad \varepsilon < \frac{\Delta}{|E| + \Delta}. \quad (15)$$

The perturbation types that make homophily rise are adding intra-class edges and removing inter-class edges. In addition to adding inter-class edges, another way to make homophily decrease is to remove intra-class edges. To avoid manufactured decisions on which type of perturbation to adopt in each iteration, we propose a homophily-restricted attack loss to replace the original attack loss in Equation 4. Our proposed attack loss is expressed as:

$$\begin{aligned} \mathcal{L}_{atk} &= -\mathcal{L}_{ce} = \frac{1}{N} \sum_{v_i} y_i \log P(y_i | f_{\theta^{(t)}}(v_i)), \\ \mathcal{L}_H &= \left( \frac{\|AH\|_0}{\|A\|_0} - \frac{\|A^{(t)}H\|_0}{\|A^{(t)}\|_0} \right)^2, \\ \lambda_1 &= \left( 1 - \frac{h_{\hat{Y}}(A) - h_{\hat{Y}}(A^{(t)})}{\varepsilon h_{\hat{Y}}(A)} \right)^2, \\ \lambda_2 &= \left( \frac{h_{\hat{Y}}(A) - h_{\hat{Y}}(A^{(t)})}{\varepsilon h_{\hat{Y}}(A)} \right)^2, \\ \mathcal{L}_{atk-hr} &= \lambda_1 \cdot \mathcal{L}_{atk} + \lambda_2 \cdot \mathcal{L}_H. \end{aligned} \quad (16)$$

We introduce Equation 16 part by part.  $P(y_i | f_{\theta^{(t)}}(v_i))$  represents the confidence level of the surrogate model's prediction on the label class for node  $v_i$ , and  $\mathcal{L}_{ce}$  represents the cross-entropy loss.  $\mathcal{L}_H$  is the loss term to restrict graph homophily, where  $H \in N \times N$  represents the label consistency between nodes. If node  $v_i$  and node  $v_j$  have the same label, then  $H_{ij} = 1$ , otherwise  $H_{ij} = 0$ .  $H$  is calculated by the pseudo-label  $\hat{Y}$ . The  $\|AH\|_0$  indicates the number of intra-class edges in the graph, and  $\|A\|_0$  indicates the number of edges in the graph. Thus, term  $\frac{\|AH\|_0}{\|A\|_0}$  is the graph homophily ratio (with self-loop included). The goal of  $\mathcal{L}_H$  is to reduce the homophily difference between the original graph structure  $A$  and the perturbed structure  $A^{(t)}$  at the  $t^{th}$  iteration. It is worth noting that the attack loss does not aim to optimize the learnable parameters but aims to compute the gradients on the graph structure. Thus, for both  $\mathcal{L}_H$  and  $\mathcal{L}_{ce}$ , we are merely concerned with their gradients on the graph structure (i.e.,  $\nabla_{A^{(t)}} \mathcal{L}_H$  and  $\nabla_{A^{(t)}} \mathcal{L}_{ce}$ ).  $\lambda_1$  and  $\lambda_2$  are a pair of weight parameters. When  $h_{\hat{Y}}(A) \approx h_{\hat{Y}}(A^{(t)})$ , we have  $\lambda_1 \rightarrow 1$  and  $\lambda_2 \rightarrow 0$ , i.e., the attack at this iteration is not restricted by homophily. When  $h_{\hat{Y}}(A) - h_{\hat{Y}}(A^{(t)}) \approx \varepsilon h_{\hat{Y}}(A)$ , we have  $\lambda_1 \rightarrow 0$  and  $\lambda_2 \rightarrow 1$ , i.e., the attack loss at this iteration focus on restricting graph homophily. When  $0 < h_{\hat{Y}}(A) - h_{\hat{Y}}(A^{(t)}) < \varepsilon h_{\hat{Y}}(A)$ , the attack loss will be a compromise between the two loss terms. With the synergy of  $\lambda_1$  and  $\lambda_2$ , the decline in graph homophily can be restricted by  $\varepsilon h_{\hat{Y}}(A)$ . The attacker can achieve edge perturbations that affect homophily decline to various levels by adjusting the parameters  $\varepsilon$ . This approach also allows the attacker to trade-off between attack performance and imperceptibility (decline in graph homophily).

## 5 EXPERIMENTS

The experimental section deals with the validity of the improvements to the surrogate model we proposed in Section 4.3 and the

performance of the model under the homophily constraint, and the visualization of the propensity to attack. Our proposed method is named multi-hop aggregation attacker (MHAtk), and the version with restricted homophily is denoted as MHAtk-rh. Section 5.2 demonstrates the effectiveness of our proposed surrogate model by showing the attack performance of MHAtk in attacking general GNNs. Section 5.3 shows the attacker's attack performance under the condition of restricted homophily reduction in order to further explore the rationale of the attack as well as to enhance the imperceptibility of the attack. Section 5.4 shows the graph homophily of MHAtk-wh with baseline Meta-Self during the attack. It demonstrates the effectiveness of our proposed homophily restriction method MHAtk-rh and visualizes the well-discussed tendency of adding inter-class edges. Extended experiments are briefly discussed in Appendix ??.

**Table 1: Statistics of datasets.**

Datasets	Vertices	Edges	Classes	Features
Citeseer	3312	4732	6	3703
Cora	2708	5429	7	1433
Cora-ML	2995	8416	7	2879

### 5.1 Experimental Settings

The test scenario in this paper is a gray-box poisoning attack to reduce the classification accuracy of the test nodes in the graph dataset.

**Datasets** The datasets involved in this paper include Cora [20], Cora-ML [20], Citeseer [23]. In these datasets, the nodes' attributes are the frequency of words, and the edges represent citations. Table 1 provides the number of nodes, edges, and classes for each dataset. Consistent with existing work [14, 43], 10% of the nodes in the assortative datasets Cora, Cora-ML, and Citeseer are labeled.

**Baselines** The baselines for generating the poisoned graph include DICE [31] based on randomness and EpoAtk [14], Meta-Self [43] and Meta-Train [43] based on gradient. Baselines are detailed as follows.

**DICE:** A method that removes the intra-class edges and adds the inter-class edges randomly. It uses the pseudo-label from the surrogate model for each unlabeled node.

**EpoAtk:** In this method, an exploration strategy similar to the genetic algorithm is proposed to avoid the possible error from the gradient information.

**Meta-Self & Meta-Train:** Baseline saliency-based attackers attack using the graph structure's gradient information. The two attack models have different attack loss functions.

The attack budget is set as 5% of the number of edges in the clean graph. Since the victim models behave differently under different seeds, each set of test experiments is run ten times. Experimental results show the mean and variance of the 10 test results.

### 5.2 Attack Performance without Restricted Homophily

In this section, we show the attack performance of our attack model with the baseline attack model on general GNNs. We select GCN

**Table 2: Attack performance on general GNN models without restricted-homophily. The experimental results are presented as classification accuracy (%). The best result in each group of experiments is bolded.**

GCN	Citeseer	Cora	Cora-ML
Clean	69.90±0.44	81.73±0.33	84.00±0.39
DICE	68.98±0.43	80.94±0.46	82.50±0.40
EpoAtk	66.25±0.44	76.98±0.59	81.31±0.39
Meta-Train	65.49±0.40	76.42±0.52	78.99±0.29
Meta-Self	60.41±0.36	75.83±0.41	<b>76.23±0.29</b>
MHAtk (Ours)	<b>58.40±0.52</b>	<b>72.66±0.57</b>	77.05±0.41
GraphSage	Citeseer	Cora	Cora-ML
Clean	69.82±0.52	80.81±0.40	81.86±0.60
DICE	69.12±0.80	80.01±0.44	80.73±0.88
EpoAtk	68.84±0.46	78.94±0.85	80.24±0.67
Meta-Train	67.86±0.91	76.09±1.02	77.67±1.76
Meta-Self	60.84±0.63	74.86±0.76	76.29±1.56
MHAtk (Ours)	<b>60.29±0.60</b>	<b>71.15±0.59</b>	<b>75.68±0.56</b>
H2GCN	Citeseer	Cora	Cora-ML
Clean	69.97±0.48	82.41±1.56	84.44±0.49
DICE	70.05±0.57	81.91±0.34	84.40±0.19
EpoAtk	69.92±0.41	81.51±0.33	83.64±0.14
Meta-Train	70.65±0.42	80.86±0.35	82.17±0.37
Meta-Self	<b>66.34±0.58</b>	81.68±0.31	82.93±0.32
MHAtk (Ours)	66.72±0.42	<b>77.85±2.58</b>	<b>80.05±3.58</b>

[12], GraphSage [9] and H2GCN [41] as victim models. GCN and GraphSage belong to the generic GCN model. H2GCN has better robustness to homophily because it is commonly used to process heterophily graph data. In this section, we use the model MHAtk, which does not contain the homophily restricted loss presented in Section 4.4. This experiment aims to verify the effectiveness of the multi-hop aggregation used to optimize the surrogate model proposed in Section 4.3, thus confirming that the loss of discrepancy information between nodes’ attributes due to oversmoothing affects the attacker’s judgment. Table 2 shows the experimental results of our method and baselines without restricted homophily.

Among the experiments, our proposed attack model MHAtk outperforms baselines in 7/9 test settings. When the victim model is GCN, our method performs 3.2% and 2.0% better than the second-place method on the datasets Cora and Citeseer; on Cora-ML, our method is slightly lower than the second-place method by 0.8%. When the victim model is GraphSage, our approach is comprehensively better than the baseline. Our method outperforms the second-place method by 0.5%, 3.7%, and 0.6% on Citeseer, Cora, and Cora-ML, respectively. When the victim model is H2GCN, our method is 3.0% and 2.1% above the second-place method on Cora and Cora-ML; it is slightly below the second-place method on Citeseer. Notably, our approach significantly increases the performance variance of the H2GCN model. The high variance means H2GCN shows poor performance a few times out of ten experiments. Comparing the three types of victim models, H2GCN has relatively better robustness, and GCN has relatively worse robustness.

The experiments demonstrate the effectiveness of our proposed multi-hop aggregation. The experiments indirectly validate our point in Section 4.3 and prove that oversmoothing due to information

**Table 3: Attack performance with restricted homophily. The hyperparameter  $\varepsilon$  takes a value less than the attack budget 5e-2.  $\varepsilon=1$  is equivalent to the original loss without considering homophily.  $h_{gt}$  represents the homophily ratio (without self-loop) of the perturbed or clean graph under the ground-truth label.**

MHAtk-rh	$\varepsilon$	GCN	GraphSage	H2GCN	$h_{gt}$
Citeseer	Clean	69.90	69.82	69.97	0.587
	1e-2	62.98	63.18	68.32	0.569
	2e-2	61.37	62.46	68.04	0.567
	3e-2	59.92	62.41	68.63	0.564
	4e-2	59.65	61.96	67.72	0.560
	1	58.40	60.29	66.72	0.549
Cora	Clean	81.73	80.81	82.41	0.744
	1e-2	74.79	72.48	79.75	0.727
	2e-2	74.58	71.60	79.11	0.721
	3e-2	73.89	71.84	78.17	0.716
	4e-2	73.16	71.24	78.65	0.712
	1	71.66	70.15	77.85	0.702

aggregation does attenuate the node attribute discrepancy information in the backpropagated gradient on the graph structure.

### 5.3 Attack Performance with Restricted Homophily

In this section, we evaluate MHAtk-rh, which applies the loss objective with restricted homophily proposed in Section 4.4. This experiment aims to explore the attack performance exhibited by the attacker when the decrease in homophily is constrained. Besides, it aims to make the edge perturbations more imperceptible in homophily variance. The  $\varepsilon$  is a hyperparameter used to regulate the strength of the homophily constraint. We perform an ablation study with various levels of the constant  $\varepsilon$ .

Table 3 is an ablation study showing the effect of the attack objective with homophily constraint (in Section 4.4) on graph homophily under various constant  $\varepsilon$ . Since the perturbation rate is 5% on datasets, we show the results at  $\varepsilon$  value of 1e-2, 2e-2, 3e-2, and 4e-2 (Note that the decrease in homophily is lower than the decrease in edge numbers from Equation 14). In addition to the classification accuracy on the victim models, we provide the homophily ratio  $h_{gt}$  (without self-loop) of the poisoned and clean graphs, calculated by the ground-truth labels. We obtain the following observations from the experimental results in Table 3. First, the results show that more loosely restricted  $\varepsilon$  implies a lower  $h_{gt}$ , and a lower  $h_{gt}$  implies a better attack performance. Second, the attacker still demonstrates attack performance in the most tightly constrained group ( $\varepsilon=1e-2$ ). Under this setting, on Citeseer, our model decreases the classification accuracy of the three victim models by 6.92%, 6.64%, and 1.65%, respectively, at the cost of only a 0.018 decrease in  $h_{gt}$ . On Cora, our model reduces the classification accuracy of the three victim models by 6.94%, 8.33%, and 2.66%, respectively, at the cost of a 0.017 decrease in  $h_{gt}$ .

Through the experiments, we find that the attack model still exhibits a significant attack performance despite the constraint on homophily decline. This implies that the differences between node



attributes are equally critical to the attackers in addition to graph heterophily. The experiments also confirm the effectiveness of the proposed homophily restricted attack objective for enhancing the imperceptibility of attacks.

#### 5.4 Homophily Variance during Attack Process

In this section, we visualize the attack process w/o homophily constraint and show the trend of the graph homophily as the attack proceeds. The purpose of this visualization includes 1. to verify our theory stated in Section 4.2 that saliency-based attack methods tend to add inter-class edges; 2 to study the mechanism of our proposed attack objective. To demonstrate the effect of our proposed homophily constraint attack objective, we show the trend of the homophily ratio  $h_{gt}$  calculated by the ground-truth labels. The visualization exhibit compares the homophily trends of MHAtk and MHAtk-rh during the attack.

Figure 2 shows the dynamics of the homophily ratio  $h_{gt}$  during the attack process of MHAtk and MHAtk-rh on the datasets Citeseer and Cora-ML. The green and red dashed lines represent the upper and lower limits of  $h_{gt}$  at the corresponding attack iteration. The gray dashed line indicates the  $h_{gt}$  of the unperturbed graph. It can be observed from Figure 2(a)(c) that during the MHAtk attack, the trend of graph homophily is close to the lower limits of  $h_{gt}$ . This verifies that the saliency-based edge perturbations reduce graph homophily by adding inter-class edges. The blue and red lines not wholly overlap may be due to the error between the pseudo-label and the ground-truth label. Figure 2(b)(d) are MHAtk-rh's, where the homophily constraint  $\epsilon$  is set to 0.02 (smaller  $\epsilon$  implies more imperceptible homophily variance). In our approach,  $h_{gt}$  becomes flat after triggering a critical value. This is due to the decrease in homophily triggering the lower bound  $h - \epsilon h$  on the homophily ratio of the pseudo-label, which results in higher weights for the constraint terms and lower weights for the attack terms in the proposed attack objective. In particular, on the Cora-ML, our model almost strictly constrains the decrease of  $h_{gt}$ . This phenomenon indicates that the smaller the difference between the pseudo-label and the ground-truth, the more significant the effect of the proposed homophily constraint.

## 6 CONCLUSION

This paper first argues that saliency-based attackers tend to add the inter-class edges. We obtain a conclusion that the attack performance of saliency-based attackers is associated with the decline in graph homophily. Based on this observation, we evaluate the importance of the information of discrepancy between nodes' attributes to the attackers. However, we propose and prove that the discrepancy information between nodes decays with the information aggregation. In other words, the surrogate model appears to be oversmoothed in the aggregation process, which makes it difficult for the attacker to exploit the complete nodes' discrepancy information. To address this issue, we propose that multi-hop aggregation is more suitable for the surrogate model. Multi-hop aggregation optimizes the message passing of the surrogate model by fusing the information in various aggregation levels. This approach preserves the high-frequency to low-frequency information of the nodes in the mapping process of the surrogate model, preserving

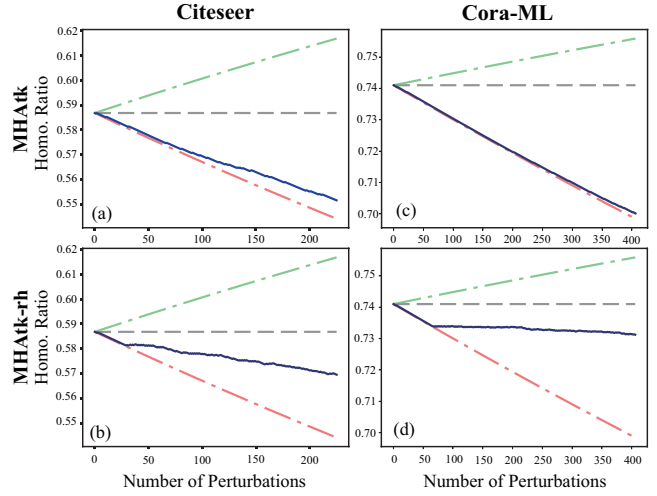


**Figure 2: The dynamics of the graph homophily ratio during the attack process of MHAtk and MHAtk-rh on the datasets Citeseer and Cora-ML. The blue line is the ground-truth homophily of the perturbed graph. The green and red lines are the upper and lower limits at the corresponding attack iteration, respectively.**

the diversity and richness of the information. On the other hand, inspired by the tendency of saliency-based attackers to add the inter-class edges, we explore the attacker's ability when subjected to restricted homophily variance. To achieve this, we propose a novel attack objective with restricted homophily. The proposed attack objective is able to control the degree of homophily constraint flexibly. This attack objective can also be used to improve the imperceptibility of saliency-based edge perturbations in terms of homophily. Experiments validated the effectiveness of our proposed methods, including improved surrogate model as well as the proposed attack objective.

## REFERENCES

- [1] Deyu Bo, Xiao Wang, Chuan Shi, and Huawei Shen. 2021. Beyond low-frequency information in graph convolutional networks. In *Proceedings of the AAAI Conference on Artificial Intelligence*, Vol. 35, 3950–3957.
- [2] Khac-Hoai Nam Bui, Jiho Cho, and Hongsuk Yi. 2021. Spatial-temporal graph neural network for traffic forecasting: An overview and open research issues. *Applied Intelligence* (2021), 1–12.
- [3] Chen Cai and Yusu Wang. 2020. A note on over-smoothing for graph neural networks. *arXiv preprint arXiv:2006.13318* (2020).
- [4] Liang Chen, Jintang Li, Jiaying Peng, Tao Xie, Zengxu Cao, Kun Xu, Xiangnan He, Zibin Zheng, and Bingzhe Wu. 2020. A Survey of Adversarial Learning on Graph. *arXiv preprint arXiv:2003.05730* (2020).
- [5] Yongqiang Chen, Han Yang, Yonggang Zhang, MA KAILI, Tongliang Liu, Bo Han, and James Cheng. 2022. Understanding and Improving Graph Injection Attack by Promoting Unnoticeability. In *International Conference on Learning Representations*.
- [6] Hanjun Dai, Hui Li, Tian Tian, Xin Huang, Lin Wang, Jun Zhu, and Le Song. 2018. Adversarial attack on graph structured data. In *International conference on machine learning*. PMLR, 1115–1124.
- [7] Simon Geisler, Tobias Schmidt, Hakan Şirin, Daniel Zügner, Aleksandar Bojchevski, and Stephan Günnemann. 2021. Robustness of graph neural networks at scale. *Advances in Neural Information Processing Systems* 34 (2021), 7637–7649.
- [8] Zhiwei Guo and Heng Wang. 2020. A deep graph neural network-based mechanism for social recommendations. *IEEE Transactions on Industrial Informatics* 17, 4 (2020), 2776–2783.



[9] William L Hamilton, Rex Ying, and Jure Leskovec. 2017. Inductive representation learning on large graphs. In *Proceedings of the 31st International Conference on Neural Information Processing Systems*. 1025–1035.

[10] Wei Jin, Yaxin Li, Han Xu, Yiqi Wang, Shuiwang Ji, Charu Aggarwal, and Jiliang Tang. 2020. Adversarial Attacks and Defenses on Graphs: A Review, A Tool and Empirical Studies. *arXiv preprint arXiv:2003.00653* (2020).

[11] Wei Jin, Yao Ma, Xiaorui Liu, Xianfeng Tang, Suhang Wang, and Jiliang Tang. 2020. Graph structure learning for robust graph neural networks. In *Proceedings of the 26th ACM SIGKDD international conference on knowledge discovery & data mining*. 66–74.

[12] Thomas N. Kipf and Max Welling. 2017. Semi-Supervised Classification with Graph Convolutional Networks. In *5th International Conference on Learning Representations, ICLR 2017, Toulon, France, April 24–26, 2017, Conference Track Proceedings*.

[13] Qimai Li, Zhichao Han, and Xiao-Ming Wu. 2018. Deeper insights into graph convolutional networks for semi-supervised learning. In *Thirty-Second AAAI conference on artificial intelligence*.

[14] Xixun Lin, Chuan Zhou, Hong Yang, Jia Wu, Haibo Wang, Yanan Cao, and Bin Xun. 2020. Exploratory Adversarial Attacks on Graph Neural Networks. In *2020 IEEE International Conference on Data Mining (ICDM)*. IEEE, 1136–1141.

[15] Meng Liu, Hongyang Gao, and Shuiwang Ji. 2020. Towards deeper graph neural networks. In *Proceedings of the 26th ACM SIGKDD international conference on knowledge discovery & data mining*. 338–348.

[16] Zihan Liu, Yun Luo, Zelin Zang, and Stan Z Li. 2022. Surrogate Representation Learning with Isometric Mapping for Gray-box Graph Adversarial Attacks. In *Proceedings of the Fifteenth ACM International Conference on Web Search and Data Mining*. 591–598.

[17] Jiaqi Ma, Shuangrui Ding, and Qiaozhu Mei. 2020. Towards more practical adversarial attacks on graph neural networks. *Advances in neural information processing systems* 33 (2020), 4756–4766.

[18] Yao Ma, Suhang Wang, Tyler Derr, Lingfei Wu, and Jiliang Tang. 2019. Attacking graph convolutional networks via rewiring. *arXiv preprint arXiv:1906.03750* (2019).

[19] Aleksander Madry, Aleksandar Makelov, Ludwig Schmidt, Dimitris Tsipras, and Adrian Vladu. 2018. Towards Deep Learning Models Resistant to Adversarial Attacks. In *International Conference on Learning Representations*.

[20] Andrew Kachites McCallum, Kamal Nigam, Jason Rennie, and Kristie Seymore. 2000. Automating the construction of internet portals with machine learning. *Information Retrieval* 3, 2 (2000), 127–163.

[21] Hongbin Pei, Bingzhe Wei, Kevin Chen-Chuan Chang, Yu Lei, and Bo Yang. 2020. Geom-GCN: Geometric Graph Convolutional Networks. In *International Conference on Learning Representations*.

[22] Chau Pham, Vung Pham, and Tommy Dang. 2020. Graph adversarial attacks and defense: An empirical study on citation graph. In *2020 IEEE International Conference on Big Data (Big Data)*. IEEE, 2553–2562.

[23] Prithviraj Sen, Galileo Namata, Mustafa Bilgic, Lise Getoor, Brian Galligher, and Tina Eliassi-Rad. 2008. Collective classification in network data. *AI magazine* 29, 3 (2008), 93–93.

[24] Daniel Smilkov, Nikhil Thorat, Been Kim, Fernanda Viégas, and Martin Wattenberg. 2017. Smoothgrad: removing noise by adding noise. *arXiv preprint arXiv:1706.03825* (2017).

[25] Lichao Sun, Yingdong Dou, Carl Yang, Ji Wang, Philip S. Yu, Lifang He, and Bo Li. 2018. Adversarial Attack and Defense on Graph Data: A Survey. *arXiv preprint arXiv:1812.10528* (2018).

[26] Yiwei Sun, Suhang Wang, Xianfeng Tang, Tsung-Yu Hsieh, and Vasant Honavar. 2019. Node injection attacks on graphs via reinforcement learning. *arXiv preprint arXiv:1909.06543* (2019).

[27] Mukund Sundararajan, Ankur Taly, and Qiqi Yan. 2017. Axiomatic attribution for deep networks. In *International conference on machine learning*. PMLR, 3319–3328.

[28] Xianfeng Tang, Yandong Li, Yiwei Sun, Huaxiu Yao, Prasenjit Mitra, and Suhang Wang. 2020. Transferring robustness for graph neural network against poisoning attacks. In *Proceedings of the 13th international conference on web search and data mining*. 600–608.

[29] Petar Velickovic, Guillem Cucurull, Arantxa Casanova, Adriana Romero, Pietro Lio, and Yoshua Bengio. 2017. Graph attention networks. *stat* 1050 (2017), 20.

[30] Xiaoyang Wang, Yao Ma, Yiqi Wang, Wei Jin, Xin Wang, Jiliang Tang, Caiyan Jia, and Jian Yu. 2020. Traffic flow prediction via spatial temporal graph neural network. In *Proceedings of The Web Conference 2020*. 1082–1092.

[31] Marcin Waniek, Tomasz P Michalak, Michael J Wooldridge, and Talal Rahwan. 2018. Hiding individuals and communities in a social network. *Nature Human Behaviour* 2, 2 (2018), 139–147.

[32] Huijun Wu, Chen Wang, Yuriy Tyshetskiy, Andrew Docherty, Kai Lu, and Liming Zhu. 2019. Adversarial examples on graph data: Deep insights into attack and defense. In *International Joint Conference on Artificial Intelligence*.

[33] Shiwen Wu, Fei Sun, Wentao Zhang, Xu Xie, and Bin Cui. 2020. Graph neural networks in recommender systems: a survey. *ACM Computing Surveys (CSUR)* (2020).

[34] Shu Wu, Yuyuan Tang, Yanqiao Zhu, Liang Wang, Xing Xie, and Tieniu Tan. 2019. Session-based recommendation with graph neural networks. In *Proceedings of the AAAI Conference on Artificial Intelligence*, Vol. 33. 346–353.

[35] Han Xu, Yao Ma, Hao-Chen Liu, Debayan Deb, Hui Liu, Ji-Liang Tang, and Anil K Jain. 2020. Adversarial attacks and defenses in images, graphs and text: A review. *International Journal of Automation and Computing* 17, 2 (2020), 151–178.

[36] Kaidi Xu, Hongge Chen, Sijia Liu, Pin Yu Chen, Tsui Wei Weng, Mingyi Hong, and Xue Lin. 2019. Topology attack and defense for graph neural networks: An optimization perspective. In *28th International Joint Conference on Artificial Intelligence, IJCAI 2019*. 3961–3967.

[37] Cheng Yang, Maosong Sun, Wayne Xin Zhao, Zhiyuan Liu, and Edward Y Chang. 2017. A neural network approach to jointly modeling social networks and mobile trajectories. *ACM Transactions on Information Systems (TOIS)* 35, 4 (2017), 1–28.

[38] Lingxiao Zhao and Leman Akoglu. 2019. Pairnorm: Tackling oversmoothing in gnns. *arXiv preprint arXiv:1909.12223* (2019).

[39] Jie Zhou, Ganqu Cui, Shengding Hu, Zhengyan Zhang, Cheng Yang, Zhiyuan Liu, Lifeng Wang, Changcheng Li, and Maosong Sun. 2020. Graph neural networks: A review of methods and applications. *AI Open* 1 (2020), 57–81.

[40] Dingyuan Zhu, Ziwei Zhang, Peng Cui, and Wenwu Zhu. 2019. Robust graph convolutional networks against adversarial attacks. In *Proceedings of the 25th ACM SIGKDD International Conference on Knowledge Discovery & Data Mining*. 1399–1407.

[41] Jiong Zhu, Yujun Yan, Lingxiao Zhao, Mark Heimann, Leman Akoglu, and Danaei Koutra. 2020. Beyond Homophily in Graph Neural Networks: Current Limitations and Effective Designs. *Advances in Neural Information Processing Systems* 33 (2020).

[42] Daniel Zügner, Amir Akbarnejad, and Stephan Günnemann. 2018. Adversarial attacks on neural networks for graph data. In *Proceedings of the 24th ACM SIGKDD International Conference on Knowledge Discovery & Data Mining*. 2847–2856.

[43] Daniel Zügner and Stephan Günnemann. 2019. Adversarial Attacks on Graph Neural Networks via Meta Learning. In *International Conference on Learning Representations*.

## A FOLLOW-UP ANALYSIS OF THEOREM 2

The following is the further analysis about the change of the difference between two nodes.

PROOF. Denote  $\psi(\lambda^\tau) = \sqrt{\sum_{m=1}^P [\sum_{k=1}^n \lambda_k^\tau (e_k^{(i)} - e_k^{(j)}) \tilde{X}_{km}]^2}$ , where  $\lambda^\tau = (\lambda_1^\tau, \dots, \lambda_n^\tau)$

According to Taylor Expansion

$$\psi(\lambda^{\tau+1}) - \psi(\lambda^\tau) \approx$$

$$[\nabla \psi(\lambda^\tau)]^T (\lambda^{\tau+1} - \lambda^\tau) + \frac{1}{2} (\lambda^{\tau+1} - \lambda^\tau)^T \nabla^2 \psi(\lambda^\tau) (\lambda^{\tau+1} - \lambda^\tau)$$

$$\text{Denote } \hat{X}_m^{(\tau)} = [X_i^{(\tau)} - X_j^{(\tau)}]_m = \sum_{k=1}^n \lambda_k^\tau (e_k^{(i)} - e_k^{(j)}) \tilde{X}_{km}$$

$$[\nabla \psi(\lambda^\tau)]_r = \frac{\sum_{m=1}^P \hat{X}_m^{(\tau)} (e_r^{(i)} - e_r^{(j)}) \tilde{X}_{rm}}{\sqrt{\sum_{m=1}^P (\hat{X}_m^{(\tau)})^2}}$$

$$[\nabla \psi(\lambda^\tau)]_{rs} = \frac{\sum_{m=1}^P (e_r^{(i)} - e_r^{(j)}) (e_s^{(i)} - e_s^{(j)}) \tilde{X}_{rm} \tilde{X}_{sm}}{\sqrt{\sum_{m=1}^P (\hat{X}_m^{(\tau)})^2}} - \frac{[\sum_{m=1}^P \hat{X}_m^{(\tau)} (e_r^{(i)} - e_r^{(j)}) \tilde{X}_{rm}] [\sum_{m=1}^P \hat{X}_m^{(\tau)} (e_s^{(i)} - e_s^{(j)}) \tilde{X}_{sm}]}{[\sum_{m=1}^P (\hat{X}_m^{(\tau)})^2]^{\frac{3}{2}}}$$

Thus,

$$X_{||i-j||}^{(\tau+1)} - X_{||i-j||}^{(\tau)} \approx \frac{\sum_{m=1}^P \hat{X}_m^{(\tau)} (\hat{X}_m^{(\tau+1)} - \hat{X}_m^{(\tau)})}{\sqrt{\sum_{m=1}^P (\hat{X}_m^{(\tau)})^2}} + \frac{\sum_{m=1}^P (\hat{X}_m^{(\tau+1)} - \hat{X}_m^{(\tau)})^2}{2\sqrt{\sum_{m=1}^P (\hat{X}_m^{(\tau)})^2}} - \frac{[\sum_{m=1}^P \hat{X}_m^{(\tau)} (\hat{X}_m^{(\tau+1)} - \hat{X}_m^{(\tau)})]^2}{2[\sum_{m=1}^P (\hat{X}_m^{(\tau)})^2]^{\frac{3}{2}}}$$

Notice that

$$\begin{aligned}\hat{X}_m^{(\tau+1)} - \hat{X}_m^{(\tau)} &= \sum_{k=1}^n (\lambda_k - 1) \lambda_k^\tau (e_k^{(i)} - e_k^j) \tilde{X}_{km} \\ &= \kappa \sum_{k=1}^n \lambda_k^\tau (e_k^{(i)} - e_k^j) \tilde{X}_{km} = \kappa \hat{X}_m^{(\tau)}\end{aligned}$$

Where  $\kappa$  is a constant dependent on adjacency matrix and  $\tau$

$$\kappa = \frac{\sum_{k=1}^n (\lambda_k - 1) \lambda_k^\tau (e_k^{(i)} - e_k^j) \tilde{X}_{km}}{\sum_{k=1}^n \lambda_k^\tau (e_k^{(i)} - e_k^j) \tilde{X}_{km}}$$

If  $\tau \rightarrow \infty, \kappa \rightarrow \lambda_{n-1} - 1$ , Then,

$$\begin{aligned}X_{||i-j||}^{(\tau+1)} - X_{||i-j||}^{(\tau)} &\approx \left(\kappa + \frac{\kappa^2}{2} - \frac{\kappa^2}{2}\right) \sqrt{\sum_{m=1}^p (\hat{X}_m^{(\tau)})^2} \\ &= \kappa \sqrt{\sum_{m=1}^p (\hat{X}_m^{(\tau)})^2} = \kappa X_{||i-j||}^{(\tau)}\end{aligned}$$